

# Fluctuating pulled fronts & Pomerons

Edmond Iancu<sup>1</sup>

*Service de Physique Théorique, CEA/DSM/SPhT, Unité de recherche associée au CNRS,  
CE Saclay, F-91191 Gif-sur-Yvette, France*

## Abstract.

I give a physical discussion of the influence of particle number fluctuations on the high energy evolution in QCD. I emphasize the event-by-event description and the correspondence with the problem of ‘fluctuating pulled fronts’ in statistical physics. I show that the correlations generated by fluctuations reduce the phase-space for BFKL evolution up to saturation. Because of that, the evolution ‘slows down’, and the rate for the energy increase of the saturation momentum is considerably decreased. Also, the stochastic aspects inherent in fluctuations lead to the breakdown of geometric scaling and of the BFKL approximation. Finally, I explain the diagrammatic interpretation of the particle number fluctuations as initiators of the Pomeron loops.

## 1. INTRODUCTION

Much of the recent progress in our understanding of QCD evolution at high energy has been triggered by the observations that (i) the gluon number fluctuations play an important role in the evolution towards saturation and the unitarity limit [1, 2] and (ii) the QCD evolution in the presence of fluctuations and saturation is in the same universality class as a series of problems in statistical physics, the prototype of which being the ‘reaction–diffusion’ problem [3, 2, 4].

These observations have developed into a profound and extremely fruitful correspondence between high–energy QCD and modern problems in statistical physics, which relates topics of current research in both fields, and which has already allowed us to deduce some insightful results in QCD by properly translating the corresponding results from statistical physics [2, 4].

At the same time, the recognition of the importance of fluctuations has revived the interest in the dilute regime of QCD at high energy, which has been somehow overlooked by the modern theory for gluon saturation, the Color Glass Condensate (CGC) [5, 6, 7]. As first noticed in Ref. [4], the evolution equation for the CGC effective theory (also known as the JIMWLK equation [8, 6, 9]) does not include the ‘gluon splittings’ responsible for gluon number fluctuations (see Sect. 6 below), and the same is true also for the Balitsky equations [10] which describe the equivalent evolution of the scattering amplitudes. On the other hand, the particle number fluctuations are correctly taken into account (in the limit where the number of colors  $N_c$  is large) by Mueller’s ‘color dipole’ picture [11], and in fact it was within

---

<sup>1</sup> Membre du Centre National de la Recherche Scientifique (CNRS), France.

that context that Salam has first observed, through numerical simulations [12], the dramatic role played by fluctuations in the course of the evolution.

Thus, not surprisingly, the dipole picture occupies a central role in the recent developments aiming at the inclusion of the effects of particle number fluctuations in the non-linear evolution towards saturation [4, 13, 14, 15, 16, 17, 18]. Furthermore, the dipole picture will also play a crucial role in the presentation that we shall give here, and which is largely adapted from Refs. [1, 2, 4, 14].

## 2. THE BALITSKY–KOVCHEGOV EQUATION

The simplest physical context in which one can address the study of gluon saturation is the collision between a small *color dipole* (a quark–antiquark pair in a colorless state) and a high energy hadron (the “target”). At high energy, the target wavefunction is dominated by gluons, to which couple the quark and the antiquark in the dipole. Thus, by following the evolution of the dipole scattering amplitude towards the unitarity limit, one can obtain information about the evolution of the gluon distribution in the target towards saturation.

Since the projectile has such a simple structure, it is quite easy to deduce the equation describing the evolution of the corresponding  $S$ -matrix with increasing energy. We shall denote the  $S$ -matrix element by  $\langle S(\mathbf{x}, \mathbf{y}) \rangle_\tau$ , where  $\mathbf{x}$  and  $\mathbf{y}$  are the transverse coordinates of the quark and the antiquark, respectively, and  $\tau \sim \ln s$  is the ‘rapidity’ variable, with  $s$  the total invariant energy squared. As we shall see,  $\tau$  plays the role of an ‘evolution time’ for the quantum evolution with increasing energy. Now suppose we increase  $\tau$  by a small amount  $d\tau$ . In order to compute the corresponding change in  $\langle S \rangle_\tau$ , it is more convenient to keep the rapidity of the target fixed and put the small change of rapidity into the elementary dipole. The latter then ‘evolves’, that is, it has a small probability of emitting a gluon due to this change of rapidity, which can be estimated as

$$dP = \frac{\alpha_s N_c}{2\pi^2} \mathcal{M}(\mathbf{x}, \mathbf{y}, \mathbf{z}) d^2z d\tau, \quad \mathcal{M}(\mathbf{x}, \mathbf{y}, \mathbf{z}) \equiv \frac{(\mathbf{x} - \mathbf{y})^2}{(\mathbf{x} - \mathbf{z})^2 (\mathbf{y} - \mathbf{z})^2}, \quad (2.1)$$

where  $N_c$  is the number of colors and  $\mathbf{z}$  is the transverse coordinate of the emitted gluon. In the large- $N_c$  limit, to which we shall restrict in what follows, the gluon can be effectively replaced by a zero-size  $q\bar{q}$  pair, and the gluon emission appears as the splitting of the original dipole  $(\mathbf{x}, \mathbf{y})$  into two new dipoles  $(\mathbf{x}, \mathbf{z})$  and  $(\mathbf{z}, \mathbf{y})$ .

If the emitted gluon is in the wavefunction of the dipole at the time it scatters on the target, then what scatters is a system of two dipoles. If the gluon is not in the wavefunction at the time of the scattering, it can be viewed as the “virtual” term which decreases the probability that the original quark–antiquark pair remain a simple dipole, thus compensating the probability for the two-dipole state. The whole process can be summarized into the following *evolution equation*, which has been originally derived by Balitsky [10]:

$$\frac{\partial}{\partial \tau} \langle S(\mathbf{x}, \mathbf{y}) \rangle_\tau = \frac{\bar{\alpha}_s}{2\pi} \int_{\mathbf{z}} \mathcal{M}(\mathbf{x}, \mathbf{y}, \mathbf{z}) \{ -\langle S(\mathbf{x}, \mathbf{y}) \rangle_\tau + \langle S^{(2)}(\mathbf{x}, \mathbf{z}; \mathbf{z}, \mathbf{y}) \rangle_\tau \}, \quad (2.2)$$

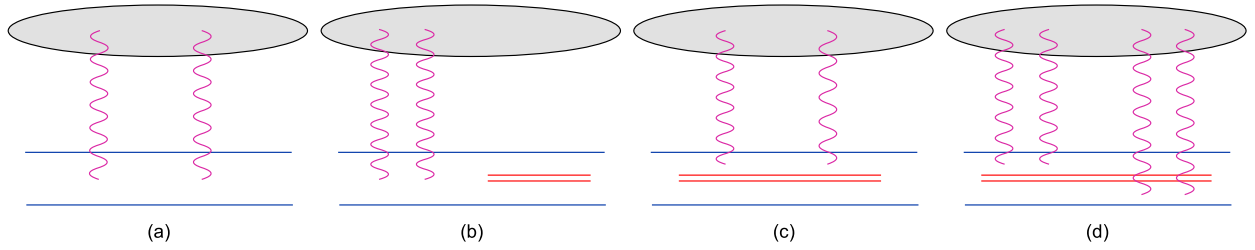


**FIGURE 1.** Diagrams for the evolution of the dipole scattering amplitude, cf. Eq. (2.3): (a) the tree-level contribution; (b) the virtual correction  $-\langle T(\mathbf{x}, \mathbf{y}) \rangle$ ; (c) the scattering of one child dipole,  $\langle T(\mathbf{x}, \mathbf{z}) \rangle$  or  $\langle T(\mathbf{z}, \mathbf{y}) \rangle$ ; (d) the simultaneous scattering of both child dipoles,  $\langle T^{(2)}(\mathbf{x}, \mathbf{z}; \mathbf{z}, \mathbf{y}) \rangle$ .

where  $\bar{\alpha}_s = \alpha_s N_c / \pi$  and  $\langle S^{(2)}(\mathbf{x}, \mathbf{z}; \mathbf{z}, \mathbf{y}) \rangle_\tau$  stands for the scattering of the two-dipole system on the target. For what follows, it is more useful to rewrite this equation in terms of the *scattering amplitude*  $T = 1 - S$ . (Indeed, we shall be mostly concerned with the weak scattering regime where  $S$  is close to one — recall that  $|S|^2$  represents the probability that no interaction take place in the collision —, and thus  $T$  is small:  $T \ll 1$ .) The corresponding equation reads:

$$\frac{\partial}{\partial \tau} \langle T(\mathbf{x}, \mathbf{y}) \rangle_\tau = \frac{\bar{\alpha}_s}{2\pi} \int_{\mathbf{z}} \mathcal{M}(\mathbf{x}, \mathbf{y}, \mathbf{z}) \left\{ -\langle T(\mathbf{x}, \mathbf{y}) \rangle_\tau + \langle T(\mathbf{x}, \mathbf{z}) \rangle_\tau + \langle T(\mathbf{z}, \mathbf{y}) \rangle_\tau - \langle T^{(2)}(\mathbf{x}, \mathbf{z}; \mathbf{z}, \mathbf{y}) \rangle_\tau \right\}, \quad (2.3)$$

and is illustrated with a few Feynman graphs in Fig. 1. (For simplicity, in this figure we represent the scattering between an elementary dipole and the target in the two-gluon exchange approximation.)

But although formally simple, Eq. (2.3) is not a closed equation — it relates a single-dipole scattering amplitude to a two-dipole one —, and the true difficulty refers to the evaluation of  $\langle T^{(2)} \rangle_\tau$ . To that aim, we need some information about the target. The simplest approximation is to assume factorization

$$\langle T^{(2)}(\mathbf{x}, \mathbf{z}; \mathbf{z}, \mathbf{y}) \rangle_\tau \approx \langle T(\mathbf{x}, \mathbf{z}) \rangle_\tau \langle T(\mathbf{z}, \mathbf{y}) \rangle_\tau, \quad (2.4)$$

which is a *mean field approximation* (MFA) for the gluon fields in the target. This immediately yields a closed, non-linear, equation for  $\langle T \rangle_\tau$ :

$$\frac{\partial}{\partial \tau} \langle T(\mathbf{x}, \mathbf{y}) \rangle_\tau = \frac{\bar{\alpha}_s}{2\pi} \int_{\mathbf{z}} \mathcal{M}(\mathbf{x}, \mathbf{y}, \mathbf{z}) \left\{ -\langle T(\mathbf{x}, \mathbf{y}) \rangle_\tau + \langle T(\mathbf{x}, \mathbf{z}) \rangle_\tau + \langle T(\mathbf{z}, \mathbf{y}) \rangle_\tau - \langle T(\mathbf{x}, \mathbf{z}) \rangle_\tau \langle T(\mathbf{z}, \mathbf{y}) \rangle_\tau \right\}. \quad (2.5)$$

This is the equation originally derived by Kovchegov [19], and commonly referred nowadays as the ‘Balitsky–Kovchegov (BK) equation’. Remarkably, this equation predicts that the scattering amplitude should approach the unitarity bound  $T = 1$  in the high energy limit. By contrast, the linear version of this equation as obtained by neglecting the term quadratic in  $\langle T \rangle_\tau$  in its r.h.s. (this is the celebrated BFKL equation [20]) predicts an exponential growth of the amplitude with  $\tau$ , which would

eventually violate unitarity. But, of course, the linear approximation breaks down when the average amplitude becomes of order one, since then the non-linear term becomes important and restores unitarity. As manifest on Fig. 1, the non-linear effects reflect *multiple scattering*.

The BK equation is perhaps the ‘best’ simple equation for dealing with the onset of unitarity in QCD at high energy and weak coupling. However, what we are primarily interested here in are the *limitations* of this equation, coming from the factorization assumption Eq. (2.4). The latter may be a good approximation if the target is a large nucleus and for not very high energies, which is the situation for which Kovchegov has originally derived this equation. More generally, this should work reasonably well when the scattering is sufficiently strong, that is, when  $\langle T \rangle_\tau$  is not much smaller than one, because in that case the external dipole scatters off a high-density gluonic system, and the *density fluctuations* are relatively unimportant. On the other, the MFA cannot be right if the scattering is *very weak*, because then the dipole is sensitive to the *dilute* part of the target wavefunction, where the fluctuations are, of course, essential. Still, given that our main interest when using Eq. (2.6) is in the *strong* scattering regime, one may expect the limitations of this equation in the dilute regime to be inessential for the problem at hand. However, this expectation turns out to be incorrect, and this is precisely what we would like to explain in what follows: The *particle number fluctuations* in the dilute regime have a strong influence, via their subsequent evolution, on the approach towards saturation and the unitarity limit.

### 3. THE FATE OF THE RARE FLUCTUATIONS

Since the fluctuations are a priori important in the weak scattering regime, we shall focus on the scattering of a *small dipole*, with transverse size  $r \equiv |\mathbf{x} - \mathbf{y}| \ll 1/Q_s(\tau)$ . We have introduced here the *saturation momentum*  $Q_s(\tau)$  [21], which is a characteristic scale of the gluon distribution in the target, and marks the scale at which a dipole scattering off the target makes the transition from weak ( $r \ll 1/Q_s$ ) to strong ( $r \gg 1/Q_s$ ) interactions. It is in fact common to *define*  $Q_s(\tau)$  by the condition

$$\langle T(\mathbf{x}, \mathbf{y}) \rangle_\tau = 1/2 \quad \text{for} \quad r = 1/Q_s(\tau), \quad (3.1)$$

and to use this condition together with the solution to the BK equation (2.6) in order to compute the energy dependence of the saturation momentum. We shall discuss more about this in the next section.

Returning to our small external dipole, we would like to relate its scattering amplitude to the average gluon density in the target. This is indeed possible in the dilute regime, since then the dipole scatters only once. In fact, at large  $N_c$  we can achieve a more symmetric description by representing also the gluons in the target as color dipoles, with an *dipole number density*  $n(\mathbf{u}, \mathbf{v})$  (for dipoles with a quark at  $\mathbf{u}$  and an antiquark at  $\mathbf{v}$ ). The external dipole  $(\mathbf{x}, \mathbf{y})$  can scatter off any of the

internal dipoles  $(\mathbf{u}, \mathbf{v})$  by exchanging two gluons. This gives:

$$\langle T(\mathbf{x}, \mathbf{y}) \rangle_\tau = \alpha_s^2 \int d^2\mathbf{u} d^2\mathbf{v} \mathcal{A}_0(\mathbf{x}, \mathbf{y}|\mathbf{u}, \mathbf{v}) \langle n(\mathbf{u}, \mathbf{v}) \rangle_\tau, \quad (3.2)$$

where  $\alpha_s^2 \mathcal{A}_0(\mathbf{x}, \mathbf{y}|\mathbf{u}, \mathbf{v})$  is the scattering amplitude for two elementary dipoles. Here, we shall not need its exact expression, but only the fact that it is *quasi-local* both with respect to the dipole *sizes* and with respect to their *impact parameters*. (The impact parameter of a dipole  $(\mathbf{x}, \mathbf{y})$  is its center-of-mass coordinate  $\mathbf{b} = (\mathbf{x} + \mathbf{y})/2$ .) This allows us to simplify Eq. (3.2) as:

$$\langle T(r, b) \rangle_\tau \simeq \alpha_s^2 \langle f(r, b) \rangle_\tau, \quad (3.3)$$

where the dimensionless quantity

$$f(r, b) \simeq r^2 \int_\Sigma d^2\mathbf{b}' n(\mathbf{r}, \mathbf{b}') \quad (3.4)$$

is the *dipole occupation number* in the target, that is, the number of dipoles with size  $r$  (per unit of  $\ln r^2$ ) within an area  $\Sigma \sim r^2$  centered at  $b$ . Eq. (3.3) shows that a small dipole projectile is a very precise analyzer of the dipole distribution in the target: the external dipoles counts the numbers of internal dipoles having the same transverse size and impact parameter as itself.

Eq. (3.3) applies so long as  $\langle T \rangle_\tau \ll 1$ , but by extrapolation it shows that unitarity corrections in the dipole-target scattering become important when the dipole occupation factor in the target becomes of order  $1/\alpha_s^2$ . This is precisely the critical density at which *saturation effects* — i.e., non-linear effects in the target wavefunction leading to the saturation of the gluon distribution — are expected to occur [11]. This argument confirms that, by studying dipole scattering in the vicinity of the unitarity limit, one has access at the physics of gluon saturation.

Let us assume an initial condition like (3.3) at the initial rapidity  $\tau_0$  and follow the evolution of the scattering amplitude with increasing  $\tau$ . At the beginning, the amplitude will rise very fast, according to the BFKL equation, but this rise will be eventually stopped by the non-linear term  $\langle T^{(2)} \rangle_\tau \equiv \langle T^{(2)}(\mathbf{x}, \mathbf{z}; \mathbf{z}, \mathbf{y}) \rangle_\tau$  in Eq. (2.3), which in the linear regime rises even faster. We have, schematically,

$$\langle T \rangle_\tau \simeq T_0 e^{\omega_{\mathbb{P}}(\tau - \tau_0)}, \quad \langle T^{(2)} \rangle_\tau \simeq T_0^{(2)} e^{2\omega_{\mathbb{P}}(\tau - \tau_0)}, \quad (3.5)$$

where  $\omega_{\mathbb{P}} = \text{const.} \times \bar{\alpha}_s$ ,  $T_0 \equiv \langle T \rangle_{\tau_0} \simeq \alpha_s^2 f_0$  and  $T_0^{(2)} \equiv \langle T^{(2)} \rangle_{\tau_0}$ . ( $f_0$  denotes the *average* occupation factor at  $\tau = \tau_0$ .) The unitarity limit is approached when  $\langle T^{(2)} \rangle_\tau \sim \langle T \rangle_\tau$ , which in turn implies  $\tau \sim \tau_c$  with

$$e^{\omega_{\mathbb{P}}(\tau_c - \tau_0)} \sim T_0 / T_0^{(2)}. \quad (3.6)$$

So, what is the ratio  $T_0^{(2)} / T_0$ ? If one assumes the factorization property (2.4), then  $T_0^{(2)} \approx (T_0)^2$ , and therefore  $T_0^{(2)} / T_0 \approx T_0 \simeq \alpha_s^2 f_0$ . Then Eq. (3.6) implies:

$$\tau_c - \tau_0 \simeq \frac{1}{\omega_{\mathbb{P}}} \ln \frac{1}{\alpha_s^2 f_0} = \frac{1}{\omega_{\mathbb{P}}} \left( \ln \frac{1}{\alpha_s^2} + \ln \frac{1}{f_0} \right). \quad (3.7)$$

But is the MFA (2.4) a reasonable approximation for a *dilute* initial condition ? To answer this question, let us consider two physical situations: (i)  $f_0 \gg 1$  (with  $f_0 \ll 1/\alpha_s^2$  though) and (ii)  $f_0 \ll 1$ . Also, remember that  $\langle T^{(2)}(\mathbf{x}, \mathbf{z}; \mathbf{z}, \mathbf{y}) \rangle_\tau$  is the scattering amplitude for two incoming dipoles  $(\mathbf{x}, \mathbf{z})$  and  $(\mathbf{z}, \mathbf{y})$  which have similar impact factors (since they have a common leg at  $\mathbf{z}$ ) and also similar sizes (since the QCD evolution, Eq. (2.3), favors the splitting into dipoles with similar sizes).

(i) In the first case, the disk  $\Sigma \sim r^2$  at  $b$  has a high occupancy, so the two external dipoles will predominantly scatter off *different* dipoles in that disk. Then, their scatterings are largely independent, and the MFA is reasonable. The result (3.7) can thus be trusted in this case.

(ii) The statement that the *average* occupation factor  $f_0$  is much smaller than one requires an explanation. Clearly, in a *given configuration* of the target, the occupation number (3.4) is *discrete* :  $f = 0, 1, 2, \dots$  ; so, for its *average* value to be smaller than one, one needs to look at *rare configurations*. That is, if one considers the *statistical ensemble* of dipole configurations generated by the evolution up to rapidity  $\tau_0$ , then for most of these configurations  $f(r, b) = 0$ , but for a small fraction among them, of order  $f_0$ ,  $f$  is non-zero and of order one. Thus,  $f_0$  is essentially the *probability* to find a dipole with the required characteristics  $(r, b)$  in the ensemble.

Consider now the scattering problem in such a *very dilute* regime: The fact that  $T_0 \sim \alpha_s^2 f_0 \ll \alpha_s^2$  means that the incoming dipole  $(r, b)$  has a small probability  $f_0(r, b)$  to find a dipole with similar characteristics in the target, with which it then interacts with a strength  $\alpha_s^2$ . Consider now *two* incoming dipoles, with similar sizes and impact parameters: there is a small probability  $f_0(r, b)$  to find a corresponding dipole in the target, but whenever this happens, *both* external dipoles can scatter off it, with an overall strength  $\alpha_s^4$ . This gives  $T_0^{(2)} \sim \alpha_s^4 f_0 \sim \alpha_s^2 T_0$ , which is much larger than the MFA prediction  $T_0^{(2)} \sim (T_0)^2$ . The scattering of the external dipoles is now *strongly correlated*. With this estimate for  $T_0^{(2)}$ , Eq. (3.6) implies

$$\tau_c - \tau_0 \simeq \frac{1}{\omega_{\mathbb{P}}} \ln \frac{1}{\alpha_s^2}. \quad (3.8)$$

For  $f_0 \ll 1$ , this is considerably smaller than the naive estimate (3.7) based on the MFA. Thus, *by enhancing the correlations in the dilute regime, the fluctuations in the particle number significantly reduce the rapidity window for BFKL evolution.*

Moreover, at the rapidity  $\tau_c$  at which the unitarity corrections cut off the BFKL growth, Eqs. (3.5) and (3.8) imply  $\langle T \rangle_{\tau_c} \sim \langle T^{(2)} \rangle_{\tau_c} \sim f_0 \ll 1$ , in sharp contrast with the prediction of the MFA ! That is, the contribution that a *rare* fluctuation  $(r, b)$  at  $\tau = \tau_0$  can give, through its subsequent evolution, to the average amplitude  $\langle T(r, b) \rangle_\tau$  at  $\tau > \tau_0$  saturates at a value *smaller* than one (of the order of the probability  $f_0(r, b) \ll 1$  of the original fluctuation) [1]. Besides, this contribution violates the factorization assumption implicit in the BK equation [4].

But then how can the average amplitude  $\langle T(r, b) \rangle_\tau$  ever approach the unitarity limit  $\langle T \rangle_\tau = 1$  ? This is possible because, as manifest on Eq. (2.3), the evolution is *non-local* in  $r$ , that is, a dipole of size  $r$  can split also from dipoles of larger sizes  $r' \gg r$ , which in the original ensemble at  $\tau_0$  had a larger probability to exist, and thus an average occupation factor  $f_0(r', b) \geq 1$ . At  $\tau = \tau_0$ , these larger dipoles

were not ‘seen’ by the external dipole  $r$ , because of the mismatch in sizes, but their descendants of size  $r$  at rapidity  $\tau > \tau_0$  are seen, and they actually dominate the scattering as compared to the rare fluctuations discussed previously.

We conclude that the correlations in the dilute regime significantly reduce the phase-space available for the BFKL evolution of the *average* amplitude towards saturation, by eliminating the rare fluctuations  $(r, b)$  for which  $\langle f(r, b) \rangle_\tau < 1$ , or, equivalently, for which  $\langle T(r, b) \rangle_\tau < \alpha_s^2$  [1]. The limiting value  $\alpha_s^2$  is the elementary ‘*quantum*’ for the strength of  $T$  in the event-by-event description, that is, the minimal non-trivial value that a physical scattering amplitude can take in a particular event, where the dipole number is discrete [2].

In view of this, one expects the evolution to ‘slow down’ as compared to the MFA. This is confirmed by an original calculation by Mueller and Shoshi [1], using a restricted BFKL evolution, which shows that the rate for the growth of saturation momentum with the energy is considerably reduced as compared to the corresponding prediction of the BK equation. In the next section, we shall recover the result of Ref. [1] from a broader perspective, which allows one to also study the statistical features of the evolution towards saturation, through a remarkable correspondence with modern results in statistical physics [2].

## 4. FLUCTUATING PULLED FRONTS

To perform a detailed study of the influence of fluctuations on the evolution towards high density, one needs a theory for correlations like  $\langle T^{(2)} \rangle_\tau$  in the presence of fluctuations. Such a theory has been recently given (within the large- $N_c$  approximation) [4, 14, 13], and we shall briefly comment on it in the last section. But before doing that, we would like to show that some very general results concerning the effects of fluctuations can be deduced without a detailed knowledge of the microscopic dynamics, by relying on universal results from statistical physics [2].

Specifically, the only assumptions that we shall need in order to derive these results are the following: (i) the *mean field description* of the dynamics of  $\langle T \rangle_\tau$  is provided by the BK equation (2.6), and (ii) in the *event-by-event description*, the amplitude  $T$  is a discrete quantity, with step  $\Delta T \sim \alpha_s^2$ .

We start by summarizing those results about the BK equation that are needed for the present purposes. We shall neglect the impact parameter dependence of the amplitude, and write the corresponding solution as  $\langle T(r) \rangle_\tau \equiv \bar{T}_\tau(\rho)$ , where  $\rho \equiv \ln(r_0^2/r^2)$  and  $r_0$  is a scale introduced by the initial conditions at low energy. Note that small dipole sizes correspond to large values of  $\rho$ . Thus, the amplitude is small,  $\bar{T}_\tau(\rho) \ll 1$ , when  $\rho$  is sufficiently large:  $\rho \gg \bar{\rho}_s(\tau)$ , where  $\bar{\rho}_s(\tau) \equiv \ln(r_0^2 \bar{Q}_s^2(\tau))$  and  $\bar{Q}_s^2(\tau)$  denotes the saturation momentum extracted from the BK equation.

The solution  $\bar{T}_\tau(\rho)$  can be visualized as a *front* which interpolates between  $T = 1$  (the unitarity limit) at  $\rho \rightarrow -\infty$  and  $T = 0$  at  $\rho \rightarrow \infty$  [3] (see Fig. 2). Note that  $T = 1$  and  $T = 0$  are stable and, respectively, unstable fixed points of the BK equation. The transition between the two regimes occurs at  $\rho \sim \bar{\rho}_s(\tau)$ ; thus, the (logarithm of the) saturation momentum plays the role of the *position of the front*. With increasing  $\tau$ , the saturation momentum rises very fast (exponentially in  $\tau$ ),

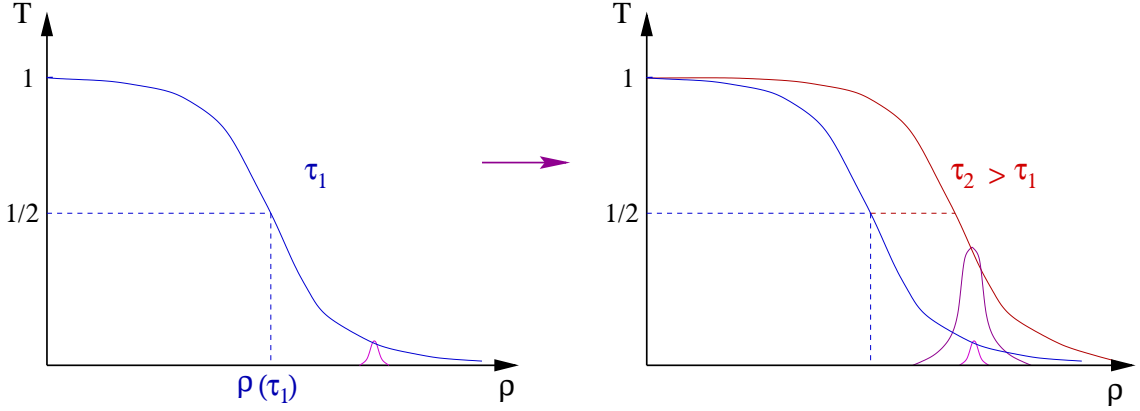


**FIGURE 2.** Evolution of the continuum front of the BK equation with increasing rapidity  $\tau$ .

so the front moves towards larger values of  $\rho$ . One finds [21, 22, 23, 24, 3]:

$$Q_s^2(\tau) \simeq Q_0^2 \frac{e^{c\bar{\alpha}_s\tau}}{(\bar{\alpha}_s\tau)^{3/2\gamma_s}}, \quad (4.1)$$

where  $Q_0^2 \propto 1/r_0^2$ , and  $c$  and  $\gamma_s$  are numbers fixed by the BFKL dynamics:  $c = 4.88\dots$  and  $\gamma_s = 0.63\dots$  Eq. (4.1) implies the following expression for the *front velocity* :

$$\bar{\lambda}(\tau) \equiv \frac{d\bar{\rho}_s(\tau)}{d\tau} \simeq c\bar{\alpha}_s - \frac{3}{2\gamma_s} \frac{1}{\tau}. \quad (4.2)$$

Its asymptotic value at large  $\tau$  represents the *saturation exponent* (the rate for the exponential growth of  $Q_s^2(\tau)$ ), here estimated in the MFA:  $\bar{\lambda}_{\text{as}} = c\bar{\alpha}_s$ .

In the weak scattering (dilute) regime at  $\rho \gg \bar{\rho}_s(\tau)$ , the form of the amplitude can be obtained by solving the linearized version of Eq. (2.6), that is, the BFKL equation. One thus finds (up to an overall normalization factor) [22, 23, 24, 3]:

$$\bar{T}_\tau(\rho) \simeq (\rho - \bar{\rho}_s) e^{-\gamma_s(\rho - \bar{\rho}_s)} \exp\left\{-\frac{(\rho - \bar{\rho}_s)^2}{2\beta\bar{\alpha}_s\tau}\right\}, \quad (4.3)$$

(with  $\beta \simeq 48.2$ ). In particular, so long as the difference  $\rho - \bar{\rho}_s$  remains much smaller than the *diffusion radius*  $\sim \sqrt{2\beta\bar{\alpha}_s\tau}$ , the Gaussian in Eq. (4.3) can be ignored, and the amplitude becomes purely a function of  $\rho - \bar{\rho}_s(\tau)$  :

$$\bar{T}_\tau(\rho) \simeq (\rho - \bar{\rho}_s(\tau)) e^{-\gamma_s(\rho - \bar{\rho}_s(\tau))} \quad \text{for} \quad \rho - \bar{\rho}_s \ll \sqrt{2\beta\bar{\alpha}_s\tau}. \quad (4.4)$$

This is the property referred to as ‘geometric scaling’ [25, 22]. It means that the front propagates without distortion, as a *traveling wave* [3].

Notice the mechanism leading to the front propagation: For a fixed  $\rho \gg \bar{\rho}_s(\tau)$ , the amplitude (4.3) rises rapidly with  $\tau$ , due to the exponential factor  $\exp(\gamma_s\bar{\rho}_s) \simeq e^{\omega_{\mathbb{P}}\tau}$  with  $\omega_{\mathbb{P}} = \gamma_s\bar{\lambda}_{\text{as}}$ ; this is the BFKL instability (see Fig. 2). Thus the front is *pulled* by the unstable (BFKL) growth of its tail at large  $\rho$ . Besides, for a given (large)



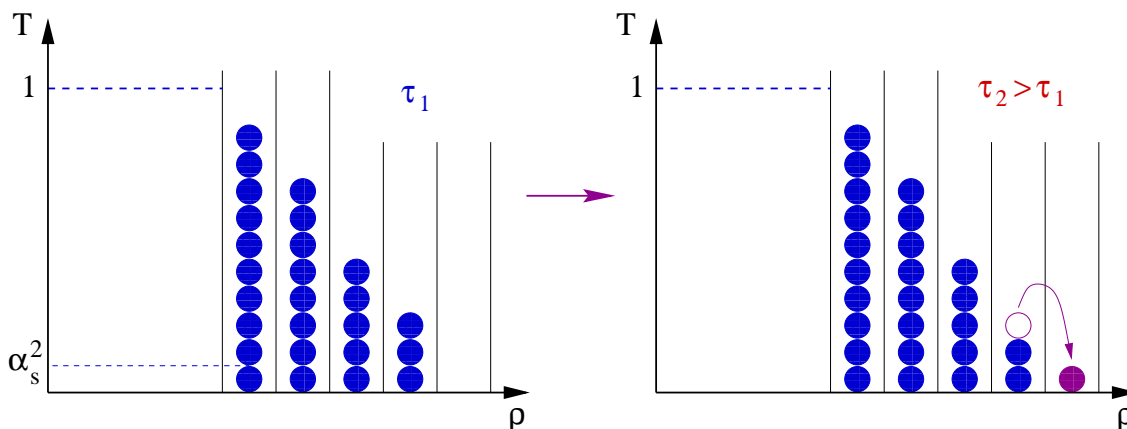


**FIGURE 3.** Evolution of the discrete front of a microscopic event with increasing rapidity  $\tau$ . The small blobs are meant to represent the elementary quanta  $\alpha_s^2$  of  $T$  in a microscopic event.

distance  $\rho - \bar{\rho}_s$  ahead of the front, the amplitude increases through *diffusion* from smaller values of  $\rho$ , until it reaches the profile (4.4) of the traveling wave.

The fact that the front corresponding to the BK equation is a *pulled front* — it propagates via the growth and spreading of small perturbations around the unstable state  $T = 0$  — is crucial for the problem at hand, as it shows that the front dynamics is driven by its *leading edge* (the front region where  $T \ll 1$ ), and therefore it might be very sensitive to *fluctuations*. Although this property has been discussed here on the basis of the linear, BFKL, equation, it turns that this is an *exact* property of the non-linear BK equation [3]. Indeed, as shown by Munier and Peschanski, the BK equation is in the same universality class as the Fisher–Kolmogorov–Petrovsky–Piscounov (FKPP) equation [26], which appears as a mean field approximation to a variety of stochastic problems in chemistry, physics, and biology, and for which the pulled front property has been rigorously demonstrated (see [27, 28] for recent reviews and more references).

Let us now return to the actual microscopic dynamics, which is *stochastic* (it includes fluctuations in the number of dipoles in the target), and where the scattering amplitude (in a given event) is *discrete*. Then, as discussed in the previous section, one needs to consider a *statistical ensemble of configurations*, which correspond to different realizations of the same evolution. To any of these configurations one can associate a front  $T_\tau(\rho)$ , which characterizes the scattering between that particular configuration and external dipoles of arbitrary size  $\rho$ .

As in the mean field case, the evolution of a configuration is described as the propagation of the associated front towards larger values of  $\rho$ . What is however new is that, because of discreteness, a microscopic front looks like a *histogram*: both  $T_\tau$  and  $\rho$  are now discrete quantities, with steps  $\Delta T = \alpha_s^2$  and  $\Delta \rho = 1$ , respectively. Because of that, the front is necessarily *compact* — for any  $\tau$ , there is only a finite number of bins in  $\rho$  ahead of  $\rho_s$  where  $T_\tau$  is non-zero (see Fig. 3) —, and this property turns out to have dramatic consequences for the propagation of the front:

In the empty bins on the right of the front tip, the local, BFKL, growth is not possible anymore (this would require a seed!). Thus, the only way for the front to

progress there is via *diffusion*, i.e., via radiation from the occupied bins at  $\rho < \rho_{\text{tip}}$  (see Fig. 3). But since diffusion is less effective than the local growth, we expect the velocity of the front — which is also the saturation exponent — to be reduced for the microscopic front as compared to the front of the MFA. The difference between the mechanisms for front propagation in the MFA and in a microscopic event can be also appreciated by comparing Figs. 2 and 3.

The extreme sensitivity of the pulled fronts to small fluctuations has been recognized in the context of statistical physics only in the recent years, first via numerical simulations for discrete particle models, then also through analytic arguments and physical considerations [29], that we have adapted to QCD in [2]. The discrete particle version of a pulled front is generally referred to as a “*fluctuating pulled front*” [27, 28]. The most striking feature of such a system is that the convergence towards the mean field limit is extremely slow, *logarithmic* in the maximal occupation number  $N$ . (For QCD,  $N \sim 1/\alpha_s^2$ , as explained after Eq. (3.4).) Specifically, if  $\lambda_N$  denotes the (asymptotic) velocity of the microscopic front for a finite value of  $N$ , and  $\lambda_\infty$  is the respective velocity in the MFA (which corresponds to the limit  $N \rightarrow \infty$ ), then for  $N \gg 1$  one finds:  $v_N \simeq v_0 - \mathcal{C}/\ln^2 N$ , where  $\mathcal{C}$  is a constant.

An analytic argument which explains this slow convergence, and allows one to compute the coefficient  $\mathcal{C}$ , has been given by Brunet and Derrida [29]. Rather than reproducing the original derivation from Ref. [29], we prefer to present (directly for the case of QCD) a qualitative argument [2] which explains the most salient feature of their result, namely its slow convergence to the mean field limit as  $N \rightarrow \infty$ .

This is related to the fact that, as mentioned before, the microscopic front has a compact width, and therefore its evolution is frozen in a state of ‘pre-asymptotic velocity’ [2]. The *width* of the front is the distance  $\Delta\rho_f = \rho - \rho_s$  over which the amplitude  $T_\tau(\rho)$  decreases from  $T_\tau(\rho_s) \sim 1$  down the minimal allowed value  $T \sim \alpha_s^2$ . This can be estimated by using the mean field expression (4.4) for the amplitude. Indeed, the MFA becomes appropriate (for a single front) as soon as  $T \gg \alpha_s^2$ , that is, everywhere except in the few bins nearby the tip of the front. But since the front is relatively wide (see below), one can neglect the tip region when estimating its width. Then Eq. (4.4) implies  $\Delta\rho_f \sim (1/\gamma_s) \ln(1/\alpha_s^2)$ , which is large indeed.

Now, from the discussion after Eq. (4.4), we know that the front sets in diffusively, and thus requires a formation ‘time’: Eq. (4.3) shows that, for the front to spread over a given distance  $\rho - \rho_s$ , it takes a rapidity evolution

$$\bar{\alpha}_s \tau \sim \frac{(\rho - \rho_s)^2}{2\beta}. \quad (4.5)$$

Through this evolution, the velocity of the front increases towards its asymptotic value according to Eq. (4.2). If the front is allowed to extend arbitrarily far away, as it was the case for the MFA, then the velocity will asymptotically approach the value  $\bar{\lambda}$ . However, when the front is compact, as for the discrete system, the formation time is finite as well, namely of the order

$$\bar{\alpha}_s \Delta\tau \sim \frac{(\Delta\rho_f)^2}{2\beta} \sim \frac{\ln^2(1/\alpha_s^2)}{2\beta\gamma_s^2}, \quad (4.6)$$

which implies that the front velocity cannot increase beyond a value

$$\lambda_{\text{as}} \simeq \bar{\lambda}_{\text{as}} - \kappa \bar{\alpha}_s \frac{\gamma_s \beta}{\ln^2(1/\alpha_s^2)}. \quad (4.7)$$

This estimate is valid when  $\alpha_s^2 \ll 1$ . The fudge factor  $\kappa$  cannot be determined by this qualitative argument, but this is computed in Refs. [29, 1] as  $\kappa = \pi^2/2$ .

The first term in Eq. (4.7) is the mean field estimate  $\bar{\lambda}_{\text{as}} \simeq 4.88\bar{\alpha}_s$ . But the second, corrective, term is particularly large, not only because it decreases very slowly with  $\alpha_s^2$ , but also because its coefficient is numerically large:  $\pi^2\gamma_s\beta/2 \approx 150$ . Thus, although Eq. (4.7) becomes an *exact result* when  $\alpha_s^2$  is arbitrarily small, this result remains useless for practical applications.

Let us finally notice that, because of the compact nature of the front, and thus of corresponding formation time, the asymptotic velocity (4.7) is reached *exponentially* fast in  $\tau$ , with a typical relaxation ‘time’ given by Eq. (4.6):  $\bar{\alpha}_s\Delta\tau \sim \ln^2(1/\alpha_s^2)$  [28]. This feature too is at variance with the MFA, where the corresponding approach is only power-like, cf. Eq. (4.2).

## 5. THE BREAKDOWN OF GEOMETRIC SCALING

In the previous subsection, we have followed a particular realization of the evolution, represented by a front  $T_\tau(\rho)$ , and we have computed the saturation exponent as the velocity of this front. Since the evolution is stochastic, different realizations of the same evolution will lead to an *ensemble* of fronts, which corresponds to the ensemble of configurations introduced in Sect. 3. The precedent discussion applies to any of these fronts: They all have the same asymptotic velocity, as given by Eq. (4.7), and except for the foremost region around the tip of the front, they all have the same shape, namely the shape predicted by the BK equation. However, in general these fronts will be displaced with respect to each other along the  $\rho$ -axis, leading to a *front dispersion*. That is, the position  $\rho_s$  of the front is itself a random variable, characterized by an expectation value  $\langle \rho_s \rangle_\tau$ , with

$$\langle \rho_s \rangle_\tau \simeq \lambda_{\text{as}}\tau, \quad \text{for} \quad \bar{\alpha}_s\tau \gg \ln^2(1/\alpha_s^2), \quad (5.1)$$

but also by a dispersion  $\sigma^2(\tau) \equiv \langle \rho_s^2 \rangle_\tau - \langle \rho_s \rangle_\tau^2$ . Physically, this dispersion originates in the rare fluctuations discussed in Sect. 3 : In a particular realization, a dipole with unusually small size may be created, which after further evolution will ‘pull’ the whole front behind him far ahead of the typical evolution, resulting in a saturation scale  $\rho_s(\tau)$  for this particular realization which is larger than the mean value  $\langle \rho_s \rangle_\tau$ .

To study the evolution of the ensemble of fronts in QCD, we shall rely again on the corresponding studies in statistical physics. These studies show that the position  $\rho_s$  of the front executes a random walk around its average value, so that the front dispersion rises linearly with  $\tau$  :

$$\sigma^2(\tau) \simeq D_{\text{fr}}\bar{\alpha}_s\tau, \quad (5.2)$$

where  $D_{\text{fr}}$  is known as the *front diffusion coefficient*. Besides, the numerical studies, which for some models have been pushed up to astronomically large values of  $N$  (as large as  $10^{160}$ ), demonstrate that  $D_{\text{fr}}$  scales like  $1/\ln^3 N$  when  $N \gg 1$  [29, 30]. So far, this is a purely numerical observation, for which there is no fundamental understanding (see however [28]). Translating this result to QCD, one finds [2]:

$$D_{\text{fr}} \simeq \frac{\mathcal{D}}{\ln^3(1/\alpha_s^2)} \quad \text{when} \quad \alpha_s \ll 1, \quad (5.3)$$

with an unknown coefficient  $\mathcal{D}$ . When decreasing  $\alpha_s$ ,  $D_{\text{fr}}$  vanishes very slowly.

This diffusive wandering of the fronts is illustrated in Fig. 4 [2]. (This applies to the discrete statistical model in Ref. [29], but a similar situation is expected also in QCD.) All the fronts represented here are different realizations of the same evolution; that is, they have been obtained by evolving the same initial condition over the same period of time. The dispersion of  $\rho_s$  is manifest in this picture, and so is also the universality of the shape of the individual fronts for  $T$ . However, precisely because of the dispersion, the shape of the *average* amplitude  $\langle T(\rho) \rangle_\tau$  (represented by the thick line in Fig. 4) is quite different from the shape of the individual fronts, and, besides, this average shape is changing with  $\tau$ : when increasing  $\tau$ , the dispersion increases, so the average front  $\langle T(\rho) \rangle_\tau$  becomes flatter and flatter, as visible on Fig. 5. We conclude that, as a consequence of fluctuations, *geometric scaling is violated for the average amplitude* [1, 2].

To study this violation in more detail, notice that the average amplitude can be computed as an *average over*  $\rho_s$ :

$$\langle T(\rho) \rangle_\tau = \int_{-\infty}^{\infty} d\rho_s P(\rho_s, \tau) T(\rho, \rho_s), \quad (5.4)$$

where  $P(\rho_s, \tau)$  is a Gaussian probability distribution for  $\rho_s$ :

$$P(\rho_s, \tau) = \frac{1}{\sqrt{\pi} \sigma(\tau)} \exp \left[ -\frac{(\rho_s - \langle \rho_s \rangle_\tau)^2}{\sigma^2(\tau)} \right], \quad (5.5)$$

and  $T(\rho, \rho_s)$  is the shape of the individual fronts, cf. Eq. (4.4), and can be schematically written as:

$$T(\rho, \rho_s) = \begin{cases} 1 & \text{for } \rho \leq \rho_s \\ \exp[-\gamma_s(\rho - \rho_s)] & \text{for } \rho \geq \rho_s. \end{cases} \quad (5.6)$$

The behaviour of the average amplitude as a function of the ‘scaling variable’  $z \equiv \rho - \langle \rho_s \rangle_\tau$  depends upon the competition between  $\sigma$  (the width of the Gaussian distribution of the fronts) and  $1/\gamma_s \sim 1$ , which characterizes the exponential decay of the individual fronts. We can thus distinguish between two types of behaviour, one at intermediate energies, the other one at high energies:

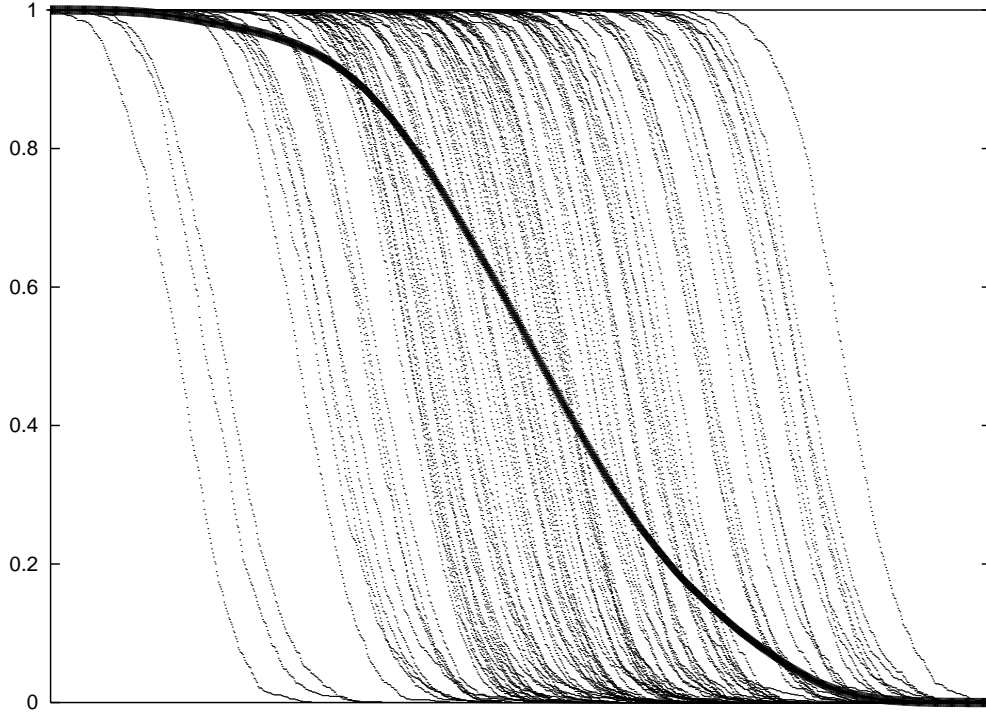


**FIGURE 4.** The scattering amplitude  $T$  for different partonic realizations at a given rapidity against  $\rho = \ln(r_0^2/r^2)$ . The thick line is the average over all realizations, i.e. the physical amplitude  $\langle T(\rho) \rangle$ , see Eq. (5.4).

- $\sigma \ll 1$

Since  $\sigma \simeq \sqrt{D_{\text{fr}} \bar{\alpha}_s \tau}$  where  $D_{\text{fr}}$  vanishes when  $\alpha_s^2 \rightarrow 0$ , one can find a regime where the diffusion of the front plays no role, and geometric scaling still holds: This happens for not too large  $\bar{\alpha}_s \tau$  and sufficiently small  $\alpha_s$ , such that  $\sigma \ll 1$ . Then one finds:

$$\langle T(\rho) \rangle_\tau \simeq \exp(-\gamma_s z) \quad \text{for} \quad z \gg \sigma. \quad (5.7)$$

That is, for a given (small)  $\alpha_s^2$ , and over a limited evolution in rapidity, the average amplitude retains the shape of the individual fronts.

- $\sigma \gg 1$

However, the typical situation at high energy is such that  $\sigma \gg 1$ . In that case, and for all values of  $z$  such that  $z \ll \sigma^2$ , one finds that  $\langle T \rangle$  is dominated by the saturating piece  $T = 1$  of Eq. (5.6), and thus is *completely insensitive* to the BFKL profile of the individual fronts. Namely:

$$\langle T \rangle_\tau \simeq \frac{1}{2} \text{Erfc} \left( \frac{z}{\sigma} \right) \quad \text{for} \quad -\infty < z \ll \sigma^2, \quad (5.8)$$

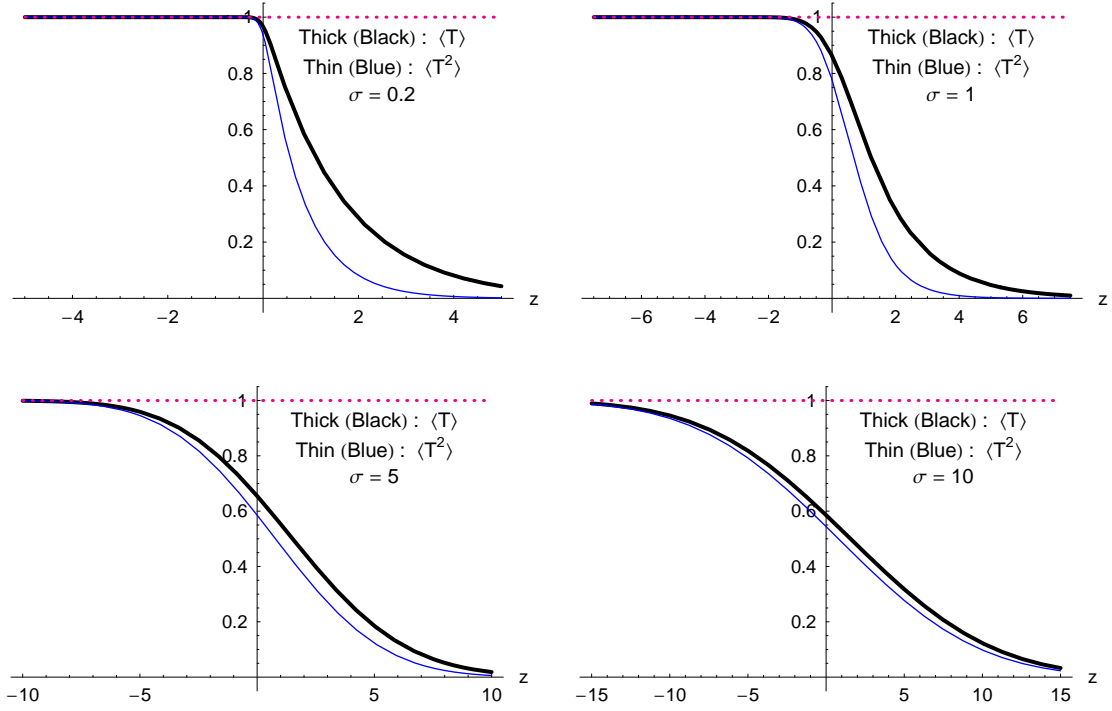


**FIGURE 5.** Evolution of  $\langle T \rangle_\tau$  and  $\langle T^2 \rangle_\tau$  with increasing  $\sigma$ .

where  $\text{Erfc}(x)$  is the complementary error function, for which we recall that

$$\text{Erfc}(x) = \begin{cases} 2 - \frac{\exp(-x^2)}{\sqrt{\pi}x} & \text{for } x \ll -1 \\ 1 & \text{for } x = 0 \\ \frac{\exp(-x^2)}{\sqrt{\pi}x} & \text{for } x \gg 1. \end{cases} \quad (5.9)$$

Eq. (5.8) shows that, in this high-energy regime, the average amplitude scales as a function of  $z/\sigma$ , that is [2]

$$\langle T(\rho) \rangle_\tau \simeq \mathcal{T} \left( \frac{\rho - \langle \rho_s \rangle_\tau}{\sqrt{\bar{\alpha}_s \tau / \ln^3(1/\alpha_s^2)}} \right), \quad (5.10)$$

which is however a *different type of scaling* as compared to the geometric scaling (compare to Eq. (4.4)): With increasing  $\tau$ , and as a function of  $z$ ,  $\langle T(z) \rangle_\tau$  becomes flatter and flatter, as illustrated in Fig. 5 [4].

The estimate (5.8) holds, in particular, in the range  $\sigma \ll z \ll \sigma^2$  where  $\langle T \rangle_\tau$  is small,  $\langle T \rangle_\tau \ll 1$ , yet is very different from the corresponding BFKL prediction (compare in this respect the expression in the last line in Eq. (5.9) to the BFKL amplitude (4.3)). To better emphasize how dramatic is the breakdown of the BFKL approximation, let us also compute the  $n$ -point correlation functions  $\langle T^{(n)} \rangle_\tau$  (at

equal points, for simplicity). One can obtain  $\langle T^n \rangle_\tau$  by simply replacing  $\gamma_s \rightarrow n\gamma_s$  in the previous formulae. Then one immediately finds that, in the high-energy regime where  $\sigma \gg 1$ , *all* the higher correlations  $\langle T^n \rangle_\tau$  are given by the *same* expression, namely by Eq. (5.8) (see also Fig. 5) [4]

$$\langle T^n \rangle_\tau \simeq \langle T \rangle_\tau \quad \text{for} \quad -\infty < z \ll \sigma^2. \quad (5.11)$$

This signals a total breakdown of the mean field approximation, except in the saturation regime where  $\langle T \rangle_\tau \simeq 1$  (see also Fig. 5). This is so because, in the presence of fluctuations and for sufficiently large  $\tau$ , average quantities like  $\langle T^{(n)} \rangle_\tau$  are dominated by those fronts within the statistical ensemble which are at saturation for the value of  $\rho$  of interest, and this even when  $\rho$  is well above the average saturation momentum  $\langle \rho_s \rangle_\tau$ , so that the corresponding *average* amplitude is small.

## 6. POMERON LOOPS

So far, our discussion has been mostly qualitative, and the language used was essentially that of statistical physics. But it is also interesting to understand these results within the more traditional language of perturbative QCD, that is, in terms of Feynman graphs and evolution equations. This is especially important in view of the limitations of the correspondence with the statistical physics, which so far has only allowed us to obtain asymptotic results (valid when  $\bar{\alpha}_s \tau \rightarrow \infty$  and  $\alpha_s^2 \rightarrow 0$ ) like Eq. (4.7). To go beyond these results, we need the actual evolution equations in QCD in the presence of both fluctuations and saturation. These equations have been constructed in the large- $N_c$  limit [4, 13, 14], by combining the Balitsky equations (or the CGC formalism) in the high density regime with the dipole picture in the dilute regime. To motivate the structure of these equations, we shall first discuss the diagrammatic interpretation of the particle number fluctuations.

We shall use, as before, the dipole picture for the target wavefunction in the dilute regime. Then, fluctuations in the dipole number appear because of the possibility that one dipole internal to the target splits into two dipoles in one step of the evolution. In the discussion of Eq. (2.3) we have already shown, in Fig. 1, the basic diagram for dipole splitting. In that discussion, the dipole appeared as the *projectile*, and the evolution was viewed as *projectile evolution* (that is, the small rapidity increment  $d\tau$  was given to the projectile). Here, we would like to visualize the relevant fluctuations as splittings of the elementary dipoles inside the target, and to that aim we need to perform *target evolution*.

In Fig. 6 we show one step in the evolution of the target, in which one of the dipoles there — the one with legs at  $\mathbf{u}$  and  $\mathbf{v}$  — has split into two new dipoles (with coordinates  $(\mathbf{u}, \mathbf{z})$  and  $(\mathbf{z}, \mathbf{v})$ , respectively). As further illustrated there, the original dipole can be probed via scattering with *one* external dipole  $(\mathbf{x}, \mathbf{y})$ , in which case it provides a contribution to the scattering amplitude  $\langle T(\mathbf{x}, \mathbf{y}) \rangle_\tau$  at the original rapidity  $\tau$ . After evolution, the two child dipoles can be measured via the scattering with *two* external dipoles, thus giving a contribution to the respective amplitude  $\langle T^{(2)}(\mathbf{x}_1, \mathbf{y}_1; \mathbf{x}_2, \mathbf{y}_2) \rangle_{\tau+d\tau}$  at rapidity  $\tau + d\tau$ . This is in agreement with

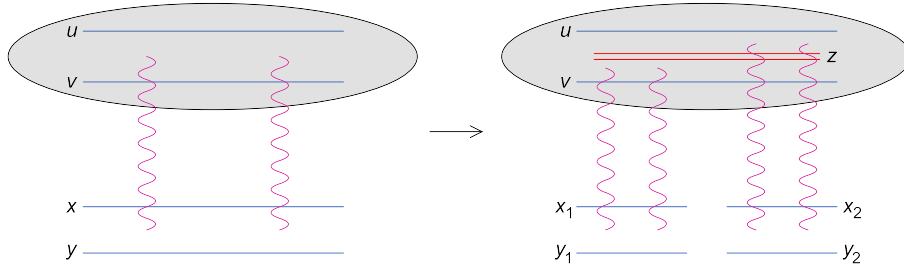


**FIGURE 6.** Diagrammatic illustration of the fluctuation term in Eq. (6.1) : the original dipole  $(\mathbf{u}, \mathbf{v})$  within the target splits at the time of the interaction into two new dipoles  $(\mathbf{u}, \mathbf{z})$  and  $(\mathbf{z}, \mathbf{v})$ , which then scatter off two external dipoles.

the discussion in Sect. 3 where we have seen that one needs to scatter two external dipoles in order to be sensitive to fluctuations.

From the previous discussion, one can also understand what should be the role of the process in Fig. 6 in the evolution of the scattering amplitudes for external dipoles: This process generates a change in the two-dipole scattering amplitude  $\langle T^{(2)} \rangle_\tau$  which is proportional to single-dipole amplitude  $\langle T \rangle_\tau$ . Specifically, the following evolution equation can be written down by inspection of Fig. 6 [14]:

$$\frac{\partial \langle T^{(2)}(\mathbf{x}_1, \mathbf{y}_1; \mathbf{x}_2, \mathbf{y}_2) \rangle_\tau}{\partial \tau} \Big|_{\text{fluct}} = \left( \frac{\alpha_s}{2\pi} \right)^2 \frac{\bar{\alpha}_s}{2\pi} \int_{\mathbf{u}, \mathbf{v}, \mathbf{z}} \mathcal{M}(\mathbf{u}, \mathbf{v}, \mathbf{z}) \mathcal{A}_0(\mathbf{x}_1, \mathbf{y}_1 | \mathbf{u}, \mathbf{z}) \mathcal{A}_0(\mathbf{x}_2, \mathbf{y}_2 | \mathbf{z}, \mathbf{v}) \times \nabla_{\mathbf{u}}^2 \nabla_{\mathbf{v}}^2 \langle T(\mathbf{u}, \mathbf{v}) \rangle_\tau. \quad (6.1)$$

The r.h.s. of this equation should be read as follows: A dipole  $(\mathbf{u}, \mathbf{v})$  from the target splits into two new dipoles  $(\mathbf{u}, \mathbf{z})$  and  $(\mathbf{z}, \mathbf{v})$  with probability  $(\bar{\alpha}_s/2\pi)\mathcal{M}(\mathbf{u}, \mathbf{v}, \mathbf{z})$  (cf. Eq. (2.1)), then the two child dipoles scatter off the external dipoles, with an amplitude  $\alpha_s^2 \mathcal{A}_0$  for each scattering. Finally, the ‘amputated’ amplitude  $(1/\alpha_s^2) \nabla_{\mathbf{u}}^2 \nabla_{\mathbf{v}}^2 \langle T(\mathbf{u}, \mathbf{v}) \rangle_\tau$  is, up to a normalization factor, the dipole density  $\langle n(\mathbf{u}, \mathbf{v}) \rangle_\tau$  in the target, as obtained by inverting Eq. (3.2).

As indicated in the l.h.s. of Eq. (6.1), this equation describes only that contribution to the evolution of  $\langle T^{(2)} \rangle_\tau$  which is associated with fluctuations in the dipole number. In addition to that, there are standard terms describing the BFKL evolution and the unitarity corrections [10, 6].

Let us finally consider the evolution of the dipole scattering amplitude  $\langle T \rangle$  after *two* steps. This involves several processes, but the most interesting among them is the one displayed in Fig. 7, which is sensitive to both fluctuations and saturation. Specifically, the first step of the evolution is the same as in Fig. 6: one dipole in the target wavefunction splits into two, which implies that the original  $\langle T \rangle$  evolves into a  $\langle T^{(2)} \rangle$  (cf. Eq. (6.1)). In the second step, the  $\langle T^{(2)} \rangle$  evolves back into a  $\langle T \rangle$ , according to the non-linear term in Eq. (2.3). The latter process has been already represented from the perspective of projectile evolution in Fig. 1.d. In the lower half part of Fig. 7, this process is now represented as target evolution: From this perspective, it describes the merging of four gluons into two.



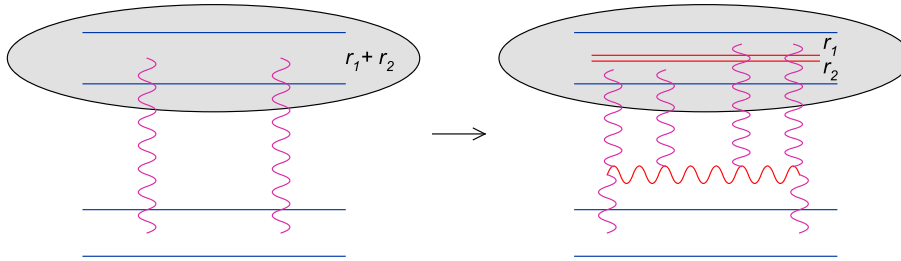


**FIGURE 7.** Two steps in the evolution of the average scattering amplitude of a single dipole: the original amplitude (left) and the Pomeron loop generated after two steps (right).

Altogether, the two-step evolution depicted in Fig. 7 generates the simplest *Pomeron loop*, where by ‘Pomeron’ we mean at this level the two-gluon exchange between two dipoles (but subsequent evolution will turn such two-gluon exchanges into BFKL pomerons). The loop is constructed with two ‘triple-Pomeron vertices’ (the dipole kernels  $\bar{\alpha}_s \mathcal{M}$ ) and two ‘Pomeron propagators’ (the dipole-dipole scattering amplitudes  $\alpha_s^2 \mathcal{A}_0$ ). It turns out that these are the same vertices as those describing the merging and splitting of *BFKL Pomerons* within perturbative QCD [31, 32, 33]. A simple effective theory for Pomeron dynamics which combines all these ingredients — the BFKL evolution of the Pomerons together with their interactions: dissociation (one Pomeron splitting into two) and recombination (two Pomerons merging into one) — and reproduces the correct evolution equations in QCD at large  $N_c$  [4, 13, 14] has been proposed in Ref. [17]. In particular, in Ref. [17] one can find an explicit expression for the Pomeron loop in Fig. 7.

In Sect. 4, we have mentioned that the BK equation — which, we recall, is a mean field approximation to the QCD evolution at high energy — is in the same universality class as the FKPP equation of statistical physics [3]. It is interesting to mention at this point that the complete evolution in QCD at large  $N_c$ , which includes the effects of particle number fluctuations via terms like Eq. (2.1), is in the same universality class as the *stochastic FKPP equation* (sFKPP) [4] — a Langevin equation with a specific ‘noise term’ which simulates particle number fluctuations [28]. By further studying this equation (in particular, via numerical calculations), one should be able to go beyond the asymptotic results presented in Sects. 4 and 5, and find the behaviour of the scattering amplitudes in QCD for realistic values of the energy and of the coupling constant. This program is currently under way.

## REFERENCES

1. A.H. Mueller and A.I. Shoshi, *Nucl. Phys.* **B692** (2004) 175.
2. E. Iancu, A.H. Mueller, and S. Munier, *Phys. Lett.* **B606** (2005) 342.
3. S. Munier and R. Peschanski, *Phys. Rev. Lett.* **91** (2003) 232001; *Phys. Rev.* **D69** (2004) 034008; *ibid.* **D70** (2004) 077503.
4. E. Iancu and D.N. Triantafyllopoulos, “A Langevin equation for high energy evolution with Pomeron Loops”, arXiv:hep-ph/0411405.
5. L. McLerran and R. Venugopalan, *Phys. Rev.* **D49** (1994) 2233; *ibid.* **49** (1994) 3352; *ibid.* **50** (1994) 2225.

6. E. Iancu, A. Leonidov and L. McLerran, *Nucl. Phys.* **A692** (2001) 583; *Phys. Lett.* **B510** (2001) 133; E. Ferreira, E. Iancu, A. Leonidov, L. McLerran, *Nucl. Phys.* **A703** (2002) 489.
7. E. Iancu, A. Leonidov and L. McLerran, *The Colour Glass Condensate: An Introduction*, hep-ph/0202270. Published in *QCD Perspectives on Hot and Dense Matter*, Eds. J.-P. Blaizot and E. Iancu, NATO Science Series, Kluwer, 2002; E. Iancu and R. Venugopalan, *The Color Glass Condensate and High Energy Scattering in QCD*, hep-ph/0303204. Published in *Quark-Gluon Plasma 3*, Eds. R.C. Hwa and X.-N. Wang, World Scientific, 2003.
8. J. Jalilian-Marian, A. Kovner, A. Leonidov and H. Weigert, *Nucl. Phys.* **B504** (1997) 415; *Phys. Rev.* **D59** (1999) 014014; J. Jalilian-Marian, A. Kovner and H. Weigert, *ibid.* **59** (1999) 014015; A. Kovner, G. Milhano and H. Weigert, *ibid.* **62** 2000 114005.
9. H. Weigert, *Nucl. Phys.* **A703** (2002) 823.
10. I. Balitsky, *Nucl. Phys.* **B463** (1996) 99; *Phys. Rev. Lett.* **81** (1998) 2024; hep-ph/0101042.
11. A.H. Mueller, *Nucl. Phys.* **B415** (1994) 373; A.H. Mueller and B. Patel, *Nucl. Phys.* **B425** (1994) 471; A.H. Mueller, *Nucl. Phys.* **B437** (1995) 107.
12. G.P. Salam, *Nucl. Phys.* **B449** (1995) 589; *ibid.* **461** (1996) 512; A.H. Mueller and G.P. Salam, *Nucl. Phys.* **B475** (1996) 293.
13. A.H. Mueller, A.I. Shoshi and S.M.H. Wong, “*Extension of the JIMWLK equation in the low gluon density region*”, arXiv:hep-ph/0501088.
14. E. Iancu and D.N. Triantafyllopoulos, *Phys. Lett.* **B610** (2005) 253.
15. E. Levin and M. Lublinsky, “*Towards a symmetric approach to high energy evolution: generating functional with Pomeron loops*”, arXiv:hep-ph/0501173.
16. A. Kovner and M. Lublinsky, “*In pursuit of Pomeron loops: the JIMWLK equation and the Wess-Zumino term*”, arXiv:hep-ph/0501198.
17. J.-P. Blaizot, E. Iancu, K. Itakura, and D.N. Triantafyllopoulos, “*Duality and Pomeron effective theory for QCD at high energy and large  $N_c$* ”, arXiv:hep-ph/0502221.
18. E. Levin, “*High energy amplitude in the dipole approach with Pomeron loops: asymptotic solution*”, arXiv:hep-ph/0502243.
19. Yu.V. Kovchegov, *Phys. Rev.* **D60** (1999), 034008; *ibid.* **D61** (2000) 074018.
20. L.N. Lipatov, *Sov. J. Nucl. Phys.* **23** (1976) 338; E.A. Kuraev, L.N. Lipatov and V.S. Fadin, *Zh. Eksp. Teor. Fiz* **72**, 3 (1977) (*Sov. Phys. JETP* **45** (1977) 199); Ya.Ya. Balitsky and L.N. Lipatov, *Sov. J. Nucl. Phys.* **28** (1978) 822.
21. L.V. Gribov, E.M. Levin, and M.G. Ryskin, *Phys. Rept.* **100** (1983) 1.
22. E. Iancu, K. Itakura, and L. McLerran, *Nucl. Phys.* **A708** (2002) 327.
23. A.H. Mueller and D.N. Triantafyllopoulos, *Nucl. Phys.* **B640** (2002) 331.
24. D.N. Triantafyllopoulos, *Nucl. Phys.* **B648** (2003) 293.
25. A.M. Stasto, K. Golec-Biernat and J. Kwiecinski, *Phys. Rev. Lett.* **86** (2001) 596.
26. R.A. Fisher, *Ann. Eugenics* **7** (1937) 355; A. Kolmogorov, I. Petrovsky, and N. Piscounov, *Moscow Univ. Bull. Math.* **A1** (1937) 1.
27. For a recent review, see W. Van Saarloo, *Phys. Rep.* **386** (2003) 29.
28. For a recent review, see D. Panja, *Phys. Rep.* **393** (2004) 87.
29. E. Brunet and B. Derrida, *Phys. Rev.* **E56** (1997) 2597; *Comp. Phys. Comm.* **121-122** (1999) 376; *J. Stat. Phys.* **103** (2001) 269.
30. E. Moro, *Phys. Rev.* **E69** (2004) 060101(R).
31. J. Bartels and M. Wüsthoff, *Z. Phys.* **C66** (1995) 157; J. Bartels and C. Ewerz, *JHEP* **9909** (1999) 026.
32. M. Braun and G.P. Vacca, *Eur. Phys. J.* **C6** (1999) 147; R. Peschanski, *Phys. Lett.* **B409** (1997) 491; M. Braun, *Phys. Lett.* **B483** (2000) 115.
33. J. Bartels, L.N. Lipatov and G.P. Vacca, *Nucl. Phys.* **B706** (2005) 391; J. Bartels, M. Braun and G.P. Vacca, “*Pomeron vertices in perturbative QCD in diffractive scattering*”, arXiv:hep-ph/0412218.